AFRL-ML-WP-TP-2006-439

CORNER CRACK PROPAGATION IN THE PRESENCE OF RESIDUAL STRESSES (PREPRINT)

A.L. Hutson, M. Huelsman, D. Buchanan, R. John, and S. Haering

MAY 2006

STINFO COPY

**MATERIALS AND MANUFACTURING DIRECTORATE
AIR FORCE RESEARCH LABORATORY
AIR FORCE MATERIEL COMMAND
WRIGHT-PATTERSON AIR FORCE BASE, OH 45433-7750**

REPORT DOCUMENTATION PAGE

1. REPORT DATE *(DD-MM-YY)*	2. REPORT TYPE	3. DATES COVERED *(From - To)*
May 2006	Conference Paper Preprint	

4. TITLE AND SUBTITLE

CORNER CRACK PROPAGATION IN THE PRESENCE OF RESIDUAL STRESSES (PREPRINT)

5a. CONTRACT NUMBER
FA8650-04-C-5200

5b. GRANT NUMBER

5c. PROGRAM ELEMENT NUMBER
N/A

6. AUTHOR(S)

A.L. Hutson, M. Huelsman, and D. Buchanan (University of Dayton Research Institute)
R. John and S. Haering (AFRL/MLLMN)

5d. PROJECT NUMBER
M02R

5e. TASK NUMBER
30

5f. WORK UNIT NUMBER
00

7. PERFORMING ORGANIZATION NAME(S) AND ADDRESS(ES)

University of Dayton Research Institute
300 College Park
Dayton, OH 45469-01228

Metals Branch, Behavior/Life Prediction Section (AFRL/MLLMN)
Metals, Ceramics, and Nondestructive Evaluation Division
Materials and Manufacturing Directorate
Air Force Research Laboratory, Air Force Materiel Command
Wright-Patterson Air Force Base, OH 45433-7750

8. PERFORMING ORGANIZATION REPORT NUMBER

9. SPONSORING/MONITORING AGENCY NAME(S) AND ADDRESS(ES)

Materials and Manufacturing Directorate
Air Force Research Laboratory
Air Force Materiel Command
Wright-Patterson AFB, OH 45433-7750

10. SPONSORING/MONITORING AGENCY ACRONYM(S)
AFRL-ML-WP

11. SPONSORING/MONITORING AGENCY REPORT NUMBER(S)
AFRL-ML-WP-TP-2006-439

12. DISTRIBUTION/AVAILABILITY STATEMENT
Approved for public release; distribution is unlimited.

13. SUPPLEMENTARY NOTES

This work has been submitted for publication in the proceedings of the 9th International Fatigue Congress (Fatigue 2006 Proceedings), Elsevier Ltd., publisher. This paper contains color. PAO Case Number: AFRL/WS 06-0785, 22 Mar 2006.

14. ABSTRACT

A technology development program known as Engine Rotor Life Extension (ERLE) has been initiated by the United States Air Force. One of the key technologies being assessed under the ERLE program is the analysis of 3D crack propagation at critical locations in turbine engine components. These critical locations are typically shot peened requiring the ability to predict 3D crack propagation at stress concentration sites in the presence of residual stresses. Hence, a study was conducted to characterize and analyze a corner crack emanating from a notch in a Ni-base superalloy in the presence of shot-peen induced residual stresses.

Finite element analysis of the corner crack propagation was performed using 3D codes, ZENCRACK™ and FRANC3D™. Initial elastic-plastic analyses were conducted to account for plasticity-induced residual stresses at the notch. Prediction of 3D crack propagation was conducted with and without shot peening induced residual stresses for comparison with experimental results. The corner crack growth predictions correlated well with the experimental results for baseline and shot-peened specimens. Significant increase in crack growth life due to shot-peening was successfully predicted using the 3D fracture mechanics codes. The modeling of the relaxation of residual stresses due to thermal exposure and the non-linear mechanical loading was essential for accurate prediction.

15. SUBJECT TERMS
ZENCRACK™, FRANC3D™, nickel-based superalloy, life prediction, crack growth, turbine engine, shot peen

16. SECURITY CLASSIFICATION OF:

a. REPORT	b. ABSTRACT	c. THIS PAGE
Unclassified	Unclassified	Unclassified

17. LIMITATION OF ABSTRACT:
SAR

18. NUMBER OF PAGES
16

19a. NAME OF RESPONSIBLE PERSON (Monitor)
Reji John

19b. TELEPHONE NUMBER *(Include Area Code)*
N/A

i

Corner Crack Propagation in the Presence of Residual Stresses

A. L. Hutson[2], M. Huelsman[2], D. Buchanan[2], R. John[1], S. Haering[1]

ABSTRACT

A technology development program known as Engine Rotor Life Extension (ERLE) has been initiated by the United States Air Force. One of the key technologies being assessed under the ERLE program is the analysis of 3D crack propagation at critical locations in turbine engine components. These critical locations are typically shot peened requiring the ability to predict 3D crack propagation at stress concentration sites in the presence of residual stresses. Hence, a study was conducted to characterize and analyze a corner crack emanating from a notch in a Ni-base superalloy in the presence of shot-peen induced residual stresses.

Baseline (as-machined) and shot-peened double edge notch Ni-base superalloy specimens were tested under tension-tension fatigue loading at 593°C in laboratory air. The specimens were designed such that the net-section-based K_t at the notch = 1.8. Cracks were initiated from a 0.1 mm EDM (electrical discharge machining) notch placed at the notch root. The nominal shot peening intensity was 6A. Crack propagation was monitored on the notch bore and the specimen face using direct current potential difference (DCPD) *in situ* monitoring, optical inspection and acetate replication.

Finite element analysis of the corner crack propagation was performed using 3D codes, ZENCRACK™ and FRANC3D™. Initial elastic-plastic analyses were conducted to account for plasticity-induced residual stresses at the notch. Prediction of 3D crack propagation was conducted with and without shot peening induced residual stresses for comparison with experimental results. The corner crack growth predictions correlated well with the experimental results for baseline and shot-peened specimens. Significant increase in crack growth life due to shot-peening was successfully predicted using the 3D fracture mechanics codes. The modeling of the relaxation of residual stresses due to thermal exposure and the non-linear mechanical loading was essential for accurate prediction.

INTRODUCTION

The use of various surface treatments in turbine engine components is widespread, and is increasing as new methods of introducing compressive residual stresses into a component surface become available for use on a production level. Historically, shot peening was used to produce compressive residual stresses in regions of a component, such as a bolt hole or blade attachment, that were prone to crack initiation. Peening has been shown in numerous studies to extend fatigue life, and so other methods, specifically laser shock peening (LSP) and low-plasticity burnishing (LPB), have been developed more recently to provide ways of inducing deeper compressive residual stresses while limiting surface deformation and damage. However, these beneficial residual stresses have not been included in fatigue life predictions of the components on which they are used. To date the residual stresses serve only as an added factor of safety, and as such do not contribute to life extension of the component. Thus a potential exists to extend the useful life of these components without increasing the risk of component failure.

By incorporating the effects of compressive residual stresses in component fatigue life prediction, the inspection interval may be increased, since the residual stresses dramatically increase crack initiation life, and the allowable flaw size may be increased depending on the depth of the residual stress field, thereby improving the probability of detection of critically sized flaws. Before compressive residual stresses can be incorporated into component life prediction, the effect of the residual stress field must be fully characterized.

---

[1]Air Force Research Laboratory, AFRL/MLLMN, Wright Patterson AFB, OH 45433-7817
[2]University of Dayton Research Institute, Dayton, OH 45469-0128, USA

Relaxation of those stresses and the effect of that relaxation on fatigue behavior must be understood. Prediction of crack growth in the presence of the complex stress field that results from various surface treatments on geometries that simulate features in real components must be achieved. A methodology for incorporating the prediction capability into the lifing regimes for existing engine components must be developed.

The following work characterizes and models 3D crack propagation on simulated engine features with and without the surface treatments commonly used to suppress crack initiation and propagation in components. A combination of laboratory experiments and computer simulations of those experiments is used to accomplish this task. Finite Element Analysis (FEA) is used with a software package specifically designed to calculate movement of the crack front. This package, called ZENCRACK™ employs FEA through ABAQUS™ to predict the propagation of the crack front assuming linear elastic behavior without residual stresses and in the presence of residual stresses from local yielding at temperature, from machining and from shot peening. Correlation between the analyses and the experiments is discussed.

EXPERIMENTAL APPROACH

A representative Ni-base superalloy with an average grain size in the range of 10 – 20 μm was used in these experiments: Rene'88DT. Material was obtained to create laboratory test specimens from retired engine disks. To manufacture the specimens, cylindrical gage section blanks were cut from the source material, and cylindrical grip section blanks were inertia-welded to the gage section. Then, the final shape machining was performed, maintaining the weld locations within the cylindrical grip region of the final form. Wire ElectroDischarge Machining (EDM) methods were used to cut the gage section blanks from the disks and to cut the near-final form of the specimen rectangular cross-section with the edge notches, as shown in Fig. 1a. A low-stress grind (LSG) process was used to provide the final specimen finish. Some specimens were shot peened to 6A after specimen manufacture but before EDM notch machining, to represent the final surface finish and residual stress (RS) condition found in many engine applications.

The experiments performed for this work were designed to simulate fastener holes like those found in turbine engine components. A double-edge notch tension (DEN(T)) specimen geometry was selected, to prevent asymmetric loading of the specimen (Fig. 1a). The edge notches, which will be referred to as the "bore" location on the specimen, were machined to a 2.7 mm radius. At one corner of the cross-section, a small EDM notch was machined to ~ 100 μm (Fig. 1b and 2). The final specimen cross-section was 7.2 mm wide and was nominally square at the notch root, with a stress concentration, Kt, of ~ 1.8.
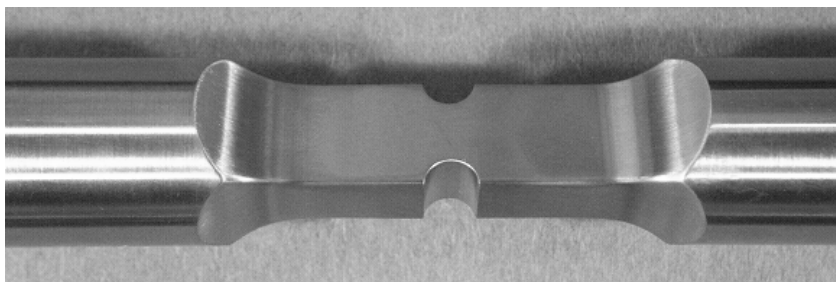

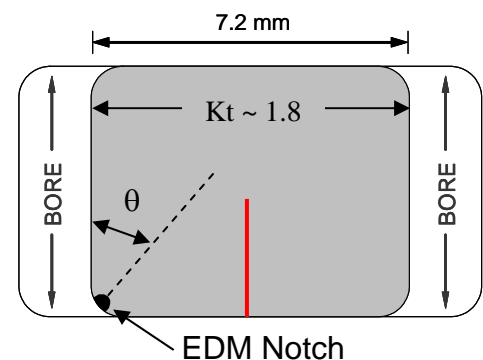Fig. 1a. Photograph of the test specimen.

Fig. 1b. Schematic of specimen cross-section at the notch root.

Experiments were performed at elevated temperature in laboratory air under constant amplitude loading at 0.33 Hz and at an applied stress ratio, R, of 0.05. Initial precrack cycles were applied at a K_{max} of 8 MPa√m under ambient conditions to provide a sharp initial crack tip with a relatively small plastic zone away from the EDM notch. The combinations of temperature and surface condition are given in Table 1. A net section stress of 680.6 MPa was used in the first experiment and corresponded to an initial stress intensity factor, K_{max}, of 25 MPa√m. This applied maximum stress was used throughout the remaining experiments.

2

Crack lengths were monitored along the specimen bore and face during each test. Direct Current Potential Difference (DCPD) was used *in situ*, and both optical and surface replication methods were used throughout to monitor surface crack lengths on the face and bore. The crack length, a, versus cycles, N, data for the various surface conditions were compared with analytical results. Once the DEN(T) specimens were fractured, optical microscopy was used to evaluate the crack front profile at the beginning of the elevated temperature portion of the test. This profile, indicated by the red line between the "RT" and "HT" regions in Fig. 2, was used as the initial crack size in the analysis discussed below.

TABLE 1
EXPERIMENT AND ANALYSIS CONDITION SUMMARY

Material	Test Temperature (°C)	Test Surface Condition	Analysis RS Condition	RS calculation
Rene'88DT	593	LSG	no residual stress	N
			bulk residual stress	Y
			bulk + LSG RS	Y
			bulk + peened RS	Y
		peened	no residual stress	N
			bulk residual stress	Y
			bulk + LSG RS	Y
			bulk + peened RS	Y

FINITE ELEMENT APPROACH

In the analysis portion of this study several models were developed for comparison with experimental results (Table 1). The first crack propagation model disregarded the effect of residual stresses. In all other analyses the residual stresses were computed in ABAQUS™ prior to executing the crack growth analysis. Separate analyses were performed incorporating bulk residual stresses that result from local yielding at the notch root, LSG residual stresses from specimen manufacture and residual stresses imposed by shot peening. Each set of analyses was conducted using the applied experimental conditions, and incorporated measured material properties including plastic deformation at elevated temperature, fatigue crack growth rates for varying stress ratios and measured residual stress profiles, where applicable.
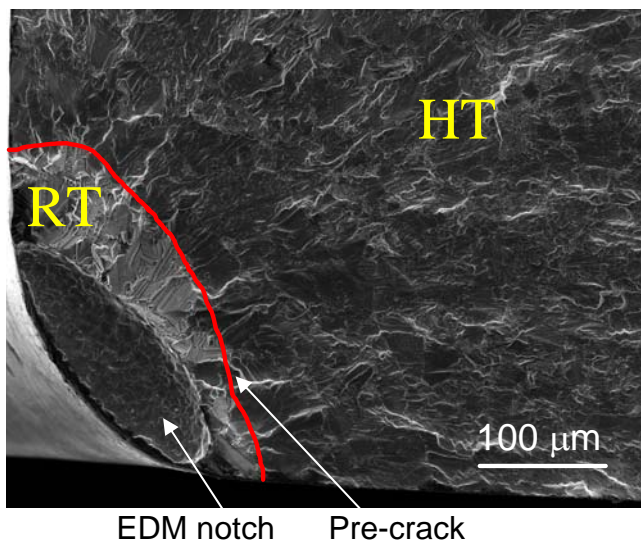

Fig. 2. Specimen fracture surface indicating EDM notch and pre-crack locations
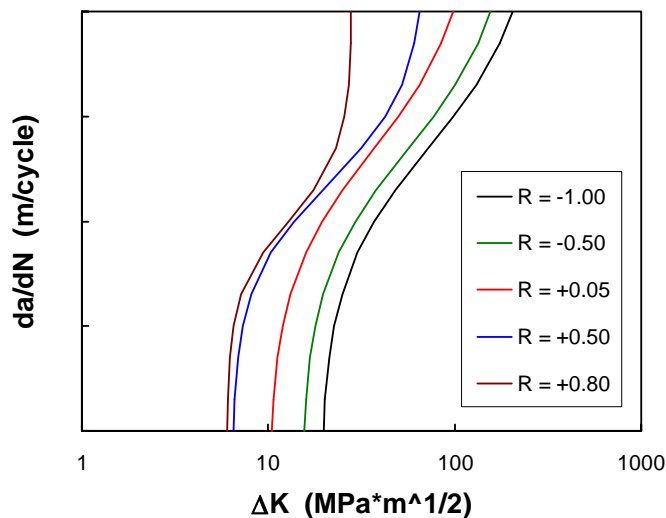

Fig. 3. FCG data used in ZENCRACK™ analyses. Data near threshold and fracture for R>0 and all data for R<0 were estimated.

Test specimen and experimental conditions were modeled as closely as possible. Dimensions prescribed in manufacture of the specimens were used to build the model geometries, including the entire grip length. Simulations of each experiment were performed using the loads and environmental conditions from the experiments and the crack front profile measured on the fracture surface that corresponded to the end of the precrack region (Fig 2). Material properties were defined based on the results of auxiliary tension and fatigue crack growth tests designed to quantify modulus, E, yield strength, YS and tensile strength, UTS, and FCG data for various applied stress ratios (Fig. 3) [1]. The data shown in Fig. 3 were required for the FCG analysis incorporating shot peened residual stresses due the compressive portion of the stress field near the specimen surface. Note that all of the data for R>0 were obtained from FCG experiments, with threshold and fracture values estimated. Data for R<0 were approximated using trends from other Ni-base superalloys [2, 3].
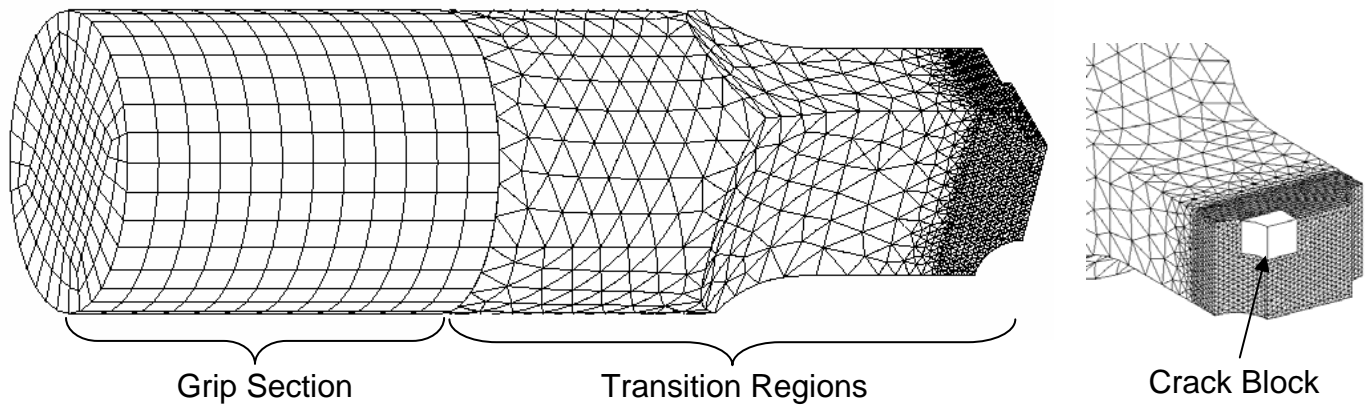

Fig. 4. DEN(T) model geometry and mesh for the ZENCRACK™ analysis.

ZENCRACK™ was used in conjunction with ABAQUS™ to perform the fatigue crack growth analysis. This application replaced a predetermined portion of a finite element model with a crack block selected by the user from a library of blocks in ZENCRACK™ [4, 5]. The crack front defined by the user is put into the new crack block mesh and then ZENCRACK™ passes the new model to ABAQUS™ for stress analysis. Once this stress analysis is completed, ZENCRACK™ takes the results, calculates K for each node along the crack front, and determines from FCG data provided by the user how far the crack should advance. ZENCRACK™ then moves the crack front nodes according to those calculations, remeshes the crack block region and creates a new ABAQUS™ model for the next step. Thus, ZENCRACK™ produces K_{max} based on energy release rate and J-integral sources, and cycle count for each crack front used in the analysis.

In the ZENCRACK™ analyses conducted for this work, the portion of the specimen grip section in contact with the test machine was used in applying the load to the virtual specimen. The total load applied to the laboratory specimen was divided by the number of nodes on the surface of the specimen corresponding to the region labeled "Grip Section" (Fig. 4). This load value was applied to each node in the grip section to produce surface tractions similar to those present in the laboratory experiment in which collet grips were used to grip and load the specimen. Symmetry about the crack plane was assumed, so that only half of the specimen needed to be modeled. In addition, the centerline of the grip section was prevented from translating parallel to the crack plane, limiting rigid body movement, and one node on the bottom outer ring of the grip section was constrained to prevent specimen rotation. Tied contact was used to join the grip section and the crack block to the transition regions. Deformation profiles were inspected to verify continuity of the tied contact during post-analysis processing.

The sq3968x16 crack block was used throughout the ZENCRACK™ crack propagation modeling [5]. This nominally cubic block is comprised of 3,968 elements and incorporates a corner crack defined by 16 elements [5]. The elements are either 8-node brick elements or 6-node wedge elements depending on the proximity of the element with respect to the crack front. Adjacent to the crack block, the geometry was meshed with 10-node tetrahedral elements that better match the edge notch and gage section contours. The grip section was composed of 8-node brick elements.

To propagate from a small corner crack to virtual specimen fracture with the appropriate level of accuracy required a three-step analysis. Although ZENCRACK™ re-meshes the crack block to advance the crack, the crack blocks all have a pre-determined number of elements, so attempting to propagate a small crack within a relatively large crack block results in a severely distorted mesh and inaccurate K predictions. This problem was addressed by entering the small initial crack (a ≈ 200 μm) into a small crack block (1.0 mm by 1.0 mm on the crack plane). When the predicted crack reached the end of this crack block, the ending crack profile was entered as the initial crack in a model that was identical to the first in all respects, except that the crack block was larger, covering nearly one fourth of the specimen cross-section (see Fig. 4). The crack from the end of the second model was entered into a third model in which the crack block included the entire specimen cross-section. Results of this multi-step analysis were truncated based on a value of $K_{fracture}$ estimated using the final crack length in the experiments, which could be measured with reasonable precision from the fracture surface due to oxidation during the elevated temperature portion of the experiments.

INCORPORATION OF RESIDUAL STRESSES

An additional uncracked model was required to determine the residual stress field for ZENCRACK™ analyses. Before the residual stresses could be entered into the ZENCRACK™ analysis, they had to be calculated for the specimen cross-section. This task was accomplished by performing an elastic-plastic stress analysis of the model without the crack block. Since the crack block was removed, symmetry about the specimen centerline could be assumed, and a model of one eighth of the specimen was used for this calculation. In the case where bulk residual stresses only were incorporated, the residual stress calculation included one full loading cycle at elevated temperature. Residual stresses were present after unloading due to yielding at the notch root; the component of stress perpendicular to the crack plane was then superimposed on the applied load in the ZENCRACK™ FCG model.
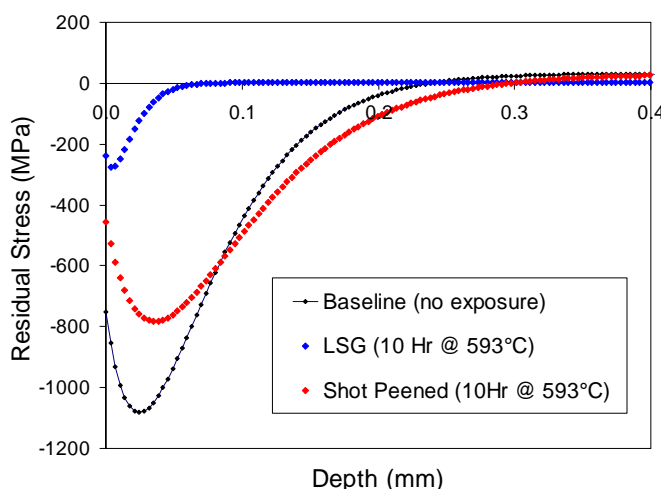

Fig. 5. Residual stress profiles: baseline (black) [7], LSG (blue) and shot-peened (red). LSG and shot-peened curves were estimated for a 10 hr exposure at 593°C.

For cases in which residual stress profiles were measured (LSG and shot-peened conditions) some additional steps were required. For the shot-peened condition, an initial baseline residual stress depth profile (shown by the black line in Fig. 5) based on measurements taken from the literature [6, 7]. The baseline profile for the LSG condition was measured from laboratory specimens. Thermal relaxation of both baseline conditions were determined from thermal exposure studies on shot peened nickel base alloys for similar temperature and exposure conditions, which have shown that the residual stress depth profile has stabilizes after 10 hours of exposure. This stabilized residual stress profile, shown in blue for LSG and red for shot-peening in Fig. 5, was used in the crack growth analysis.

This stabilized profile was entered into the uncracked finite element model via a user subroutine, and an equilibrium step was performed prior to the loading cycle at elevated temperature. The resulting stresses

5

perpendicular to the crack plane from a line running between the specimen "faces" (see red line in Fig 1b) was then compared with the measured profile. Once an acceptable match was achieved for the stress profile corresponding to the specimen center (Fig. 1b), the stresses perpendicular to the crack plane for the entire cross-section were entered into the ZENCRACK™ model and the FCG analysis was performed. The profiles produced by the equilibrium step are shown in Figs. 6 and 7 for the LSG and shot-peened residual stress profiles, respectively. These plots include the Z-component stress plotted as a function of both X and Y (corresponding to the face and bore of the specimen, respectively).
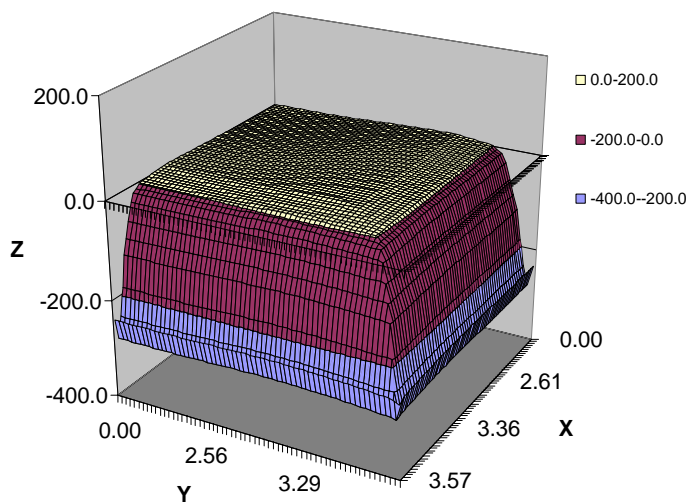

Fig. 6. Surface plot of crack opening stresses for the LSG ZENCRACK™ analysis, where X = face coordinate and Y = bore coordinate.
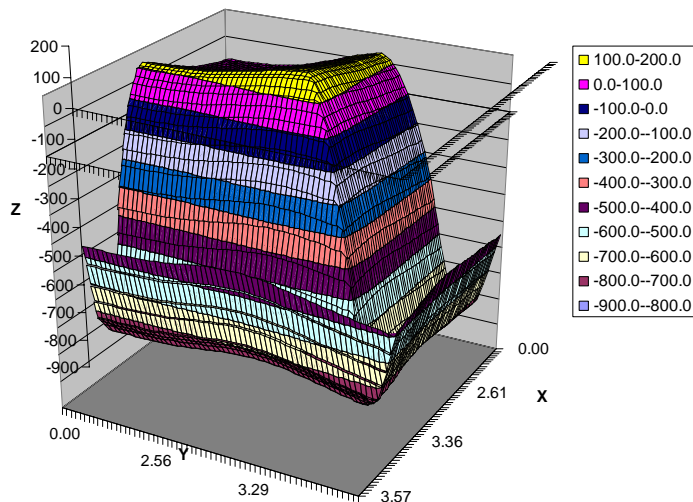

Fig. 7. Surface plot of crack opening stresses for the shot-peened ZENCRACK™ analysis, where X = face coordinate and Y = bore coordinate.

Representative residual stress field results for the LSG and shot-peened 1/8th models are shown in Fig. 8. In the figure fringe plots of the Z-component stresses are shown for both residual stress conditions after a full loading cycle has been modeled at temperature. Fig. 8a includes results for the LSG residual stress model; Fig. 8b shows results for the shot-peened model. The red region in Fig. 8a corresponds the region of the specimen where the residual stress is in tension. In Fig. 8b the red and orange regions represent the tensile portion of the residual stress field. Note the increased size of the tensile region as well as the higher magnitude for the shot-peened stresses (~150 MPa vs. ~24 MPa for the LSG condition). Once the residual stress profiles were computed, they were assumed to be static. During the ZENCRACK™ analysis, only the far field specimen load varied with time and the residual stresses were not updated as the crack front was advanced.

Fig. 8a. 3D LSG residual stress profile (1/8th model) after unloading – (red region is in tension)

Fig. 8b. 3D shot-peened residual stress profile (1/8th model) after unloading – (red and orange regions are in tension).

Another model check was performed after the crack block was inserted into the model. In the analysis with the crack block half of the total specimen was modeled, with symmetry assumed on the crack plane only. Stress profiles from these analyses were less informative, since the stress peaks at the crack tip tend to eclipse stress features of less magnitude. The most informative results were taken from deformation maps, which were used to verify continuity of the tied contacts as well as the direction of applied forces and the accuracy of other boundary conditions.

RESULTS

Comparison of ZENCRACK™ & FRANC3D™

Results of the linear elastic (LE) ZENCRACK™ analysis are shown in Figs. 9, 10 and 11 along with results from analyses performed using the boundary element analysis code, FRANC3D™ [8, 9]. Fig. 9 includes the maximum stress intensity factor, K, plotted against crack length, a, for a crack front position approximately forty-five degrees from the specimen face, corresponding to $\theta = 45°$ in Fig. 1b. Data in Figs. 10 and 11 were taken along lines corresponding to $\theta = 10°$ and $80°$, respectively. The manner in which the crack front is extended differs between the two analysis codes. ZENCRACK™ extends the crack front based on da/dN-ΔK (given in Fig. 3) at each of the seventeen crack front nodes with a given maximum crack extension, while FRANC3D™ extends the crack (Δa) proportionate to ΔK along the crack front such that

$$\Delta a = \Delta a_{max} * (\Delta K/\Delta K_{max})^n \quad\quad\quad\quad (1)$$

where n is an integer. For this work 1 and 3 were selected for n and the results compared. FRANC3D™ analyses produced comparable K vs. a results (blue and green curves) for either value of n for all three selected crack front locations. Results from the ZENCRACK™ analysis (red curves) were similar to those from the FRANC3D™ analyses, but were, in general, closer to the FRANC3D™ results using n = 3. These results provide validation of the ZENCRACK™ analyses.
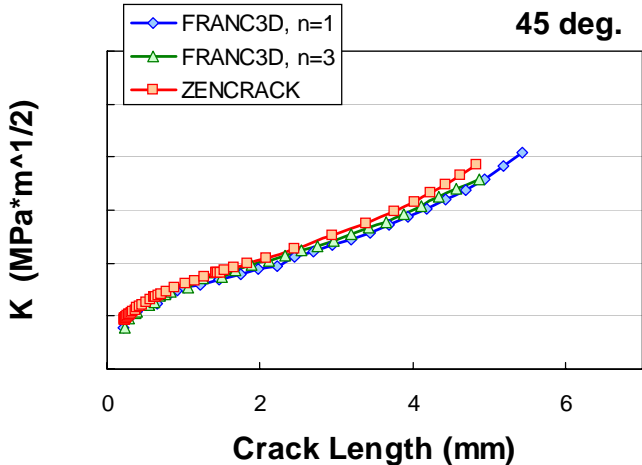

Fig. 9. K vs. a results from the ZENCRACK™ LE analysis compared with a boundary element model of the same conditions for $\theta = 45°$.
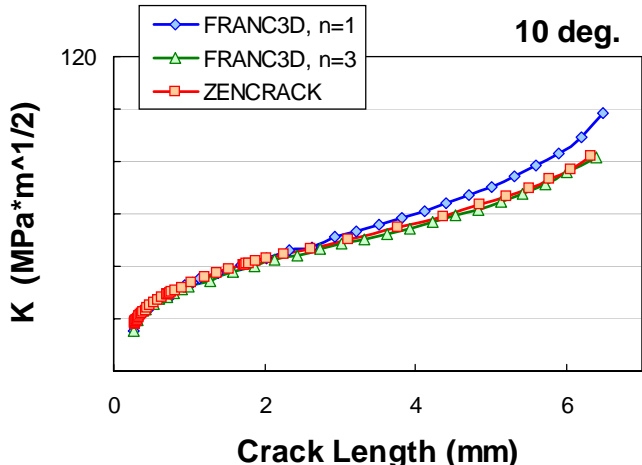
Fig. 10. K vs. a results from the ZENCRACK™ LE analysis compared with a boundary element model of the same conditions for $\theta = 10°$.

To accurately model the fatigue crack growth behavior of the test specimens, residual stresses had to be imposed in the analyses. FRANC3D™ does not have a mechanism through which the residual stresses may be introduced, but ZENCRACK™ allows user routines to be employed to define arbitrary states of stress. Thus, ZENCRACK™ was used for all of the analyses that incorporated residual stresses. As described in the previous section, LSG and shot-peened residual stresses were measured, and an equilibrium analysis step was used in a separate model to calculate the stress field imposed across the crack plane in the subsequent fatigue crack growth analysis. Bulk residual stresses were also calculated in the manner discussed above.
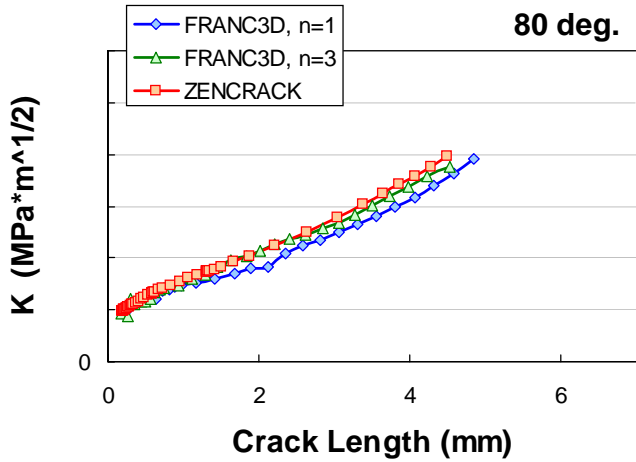
Fig. 11. K vs. a results from the ZENCRACK™ LE analysis compared with a boundary element model of the same conditions for θ = 80°.
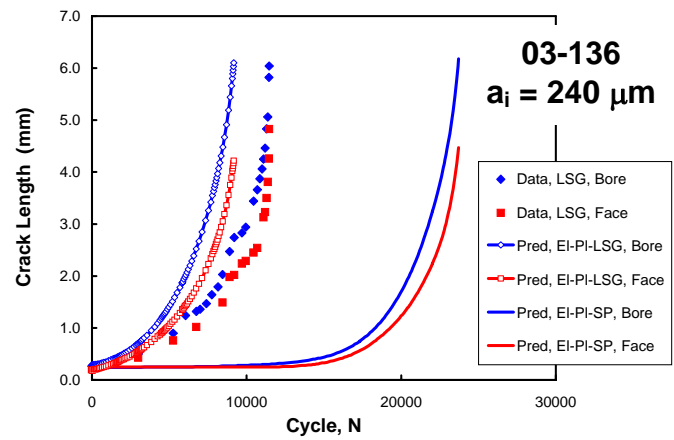

Fig. 12. Comparison of ZENCRACK™ and experimental a vs. N results for experiment with LSG residual stresses.

Crack Growth Behavior

Experiments were performed only on specimens with either LSG or shot-peening induced residual stresses. No experiments with an initially stress free surface were planned since bulk residual stresses would be produced in the first loading cycle of each experiment. All tests were conducted using nominally identical loading and environmental conditions, so the only variations from specimen to specimen were the residual stress condition and the initial crack length produced during precracking.

Data from an experiment in which the specimen was left in the LSG condition, and the associated analyses are shown in Fig. 12. This specimen, designated 03-136, had an initial crack length of ~240 μm after precracking and produced a fatigue life of 11,464 cycles. The analysis of this experiment was performed with both the LSG and shot-peened residual stresses imposed. As expected, the a vs. N curve predicted for the LSG residual stresses compares reasonably well with data from the experiments. The model that incorporated shot-peened residual stresses predicted a fatigue life nearly twice as long as occurred in the experiment for this crack size.
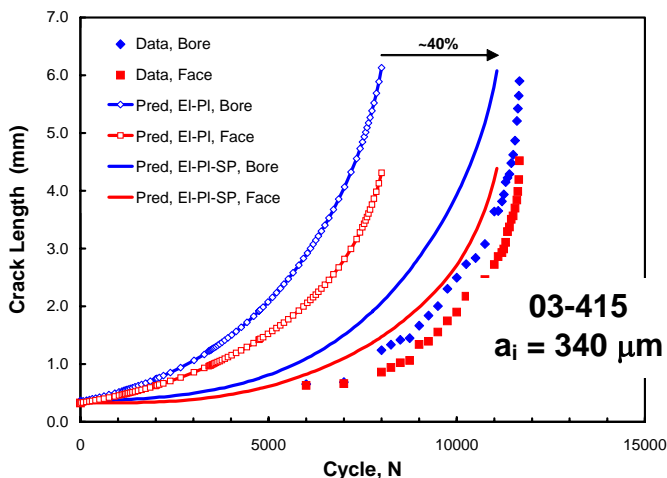

Fig. 13. Comparison of ZENCRACK™ and experimental a vs. N results for experiment with shot-peening induced residual stresses.
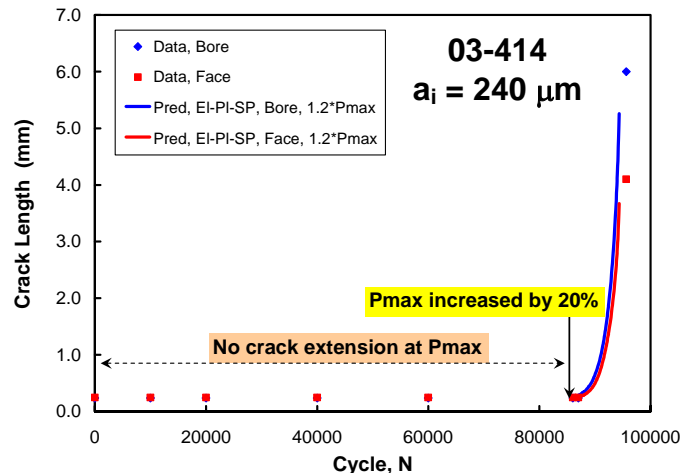

Fig. 14. Comparison of ZENCRACK™ and experimental a vs. N results for the first experiment. Stress was raised 20% to 680.6 MPa at ~85k cycles.

A shot-peened specimen, designated 03-415 was tested with a final pre-crack length of ~340 μm. The experimental results (Fig. 13) compare well with the analytical results that incorporated the shot-peening induced residual stresses. A second simulation, in which the peened residual stresses were replaced with LSG residual stresses, was also performed. Comparison of a vs. N results from the two analyses indicates an

8

increase of ~40% in fatigue life resulting from the shot-peening induced residual stresses. This value is lower than the estimated level of improvement indicated for the smaller initial crack size (~100% increase).

Results from another shot-peened specimen, designated 03-414, are shown in Fig. 14. Crack length versus cycle count data are shown here for several analyses as well as the experiment. The initial crack length was ~240 μm, and it should be noted that a lower stress was used initially. At the first stress level of 566.8 MPa, no crack propagation was measured during the ~85,000 cycles that were applied. Once the stress was increased by 20% to 680.6 MPa, the crack began to propagate, indicating the benefit of shot peening on crack behavior. The analytical simulations performed with the shot peening-induced residual stresses imposed closely match the experimental results. Larger cracks will be influenced less by the surface residual stresses, since part of the crack front lies in the tensile region of the residual stress field that balances the surface compression.

SUMMARY

The results of this study successfully demonstrated the potential to predict the effect of compressive residual stresses on crack growth retardation at corner cracks. Elevated temperature corner crack growth experiments on notched Rene`88DT specimens with low stress grind and shot-peened surface treatment were performed. Finite element models of the uncracked specimen were used to determine the residual stresses profiles from inelastic loading and surface treatment for input into the crack growth model. Separate calculations were performed incorporating LSG and shot-peened residual stresses for the crack growth analyses. The fatigue crack growth predictions with and without residual stresses correlate well with the experimental results. The analyses successfully predicted the significant increase in crack growth life due to shot peened residual stresses and indicate a greater influence on crack growth resistance for smaller cracks corresponding to the influence of residual stresses on the local K field. Fatigue crack growth predictions using ZENCRACK™ without residual stresses were validated with FRANC3D™. The methodology implemented here to incorporate residual stress depth profiles into corner crack growth analysis can be applied to other materials and geometries of interest.

ACKNOWLEDGMENTS

REFERENCES

[1]   Huron, E. S., "Serrated yielding in a nickel-base superalloy," Superalloy, 1992, pp. 675-684.

[2]   Krueger, D. D., Kissinger, R. D., and Menzies R. G., "Development and introduction of a damaged tolerant high temperature nickel-based disk alloy, Rene'88DT," Superalloys, 1998, pp. 277-286.

[3]   Van Stone, R.H. and Krueger, D.D., "Near-Threshold Crack Growth in Nickel-Base Superalloys," Fracture Mechanics: Nineteenth Symposium, ASTM STP 969, T. A. Cruse, Ed., 1988, pp. 883-906.

[4]   Chandwani, R., Cook, G., Timbrell, C., Wiehahn, M., Basu, A., Sharma, A.M. and Chakrabarti, P., Improved Life Prediction of Turbine Engine Components Using a Finite Element Based Software Called ZENCRACK™, AFRL-ML-WP-TR-2004-4014, Wright Patterson AFB, OH 45433-7750, 2003.

[5]   User Manual for ZENCRACK™ 7.1, Zentech International Ltd., Camberley, Surrey, UK, September 2003.

[6] Tufft, M. K., <u>Development of a Fracture Mechanics / Threshold behavior model to assess the effects of competing mechanisms induced by shot peening on cyclic life of a Nickel-base superalloy, Rene88DT,</u> Ph.D. Dissertation, University of Dayton, Dayton, OH, 1997.

[7] Tufft, M.K., "Modeling of Fatigue Behavior due to Shot Peening Conditions," Proceedings of the 8th International Conference on Shot Peening (ICSP-8), Garmisch-Partenkirchen, Germany, September, 2002, pp. 530-539.

[8] FRacture ANalysis Code (FRANC3D) for simulating arbitrary non-planar 3D crack growth. Available at http://www.cfg.cornell.edu/software/software.htm.

[9] Carter, B.J., Wawrzynek, P.A., and Ingraffea, A.R., "Automated 3D Crack Growth Simulation," International Journal of Numerical Methods in Engineering, Vol. 47, pp. 229-253, 2000.